Supporting Information

Effects of Graphite Structure and Ion Transport on the Electrochemical Properties of Rechargeable Aluminum–Graphite Batteries

Jeffrey H. Xu, Damon E. Turney, Ankur Jadhav, and Robert J. Messinger*

Department of Chemical Engineering, The City College of New York, CUNY, New York, New York 10031, United States

*E-mail: rmessinger@ccny.cuny.edu

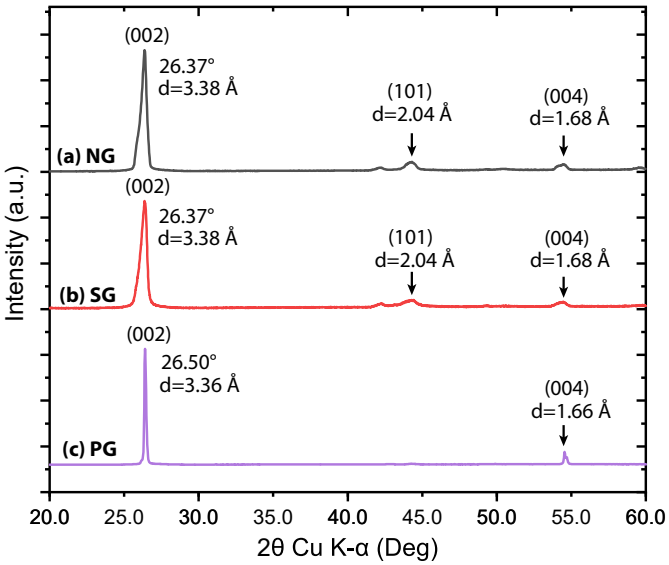

Figure S1. X-Ray diffraction (XRD) patterns for pristine (a) natural graphite (NG), (b) synthetic graphite (SG) and (c) pyrolytic graphite (PG).

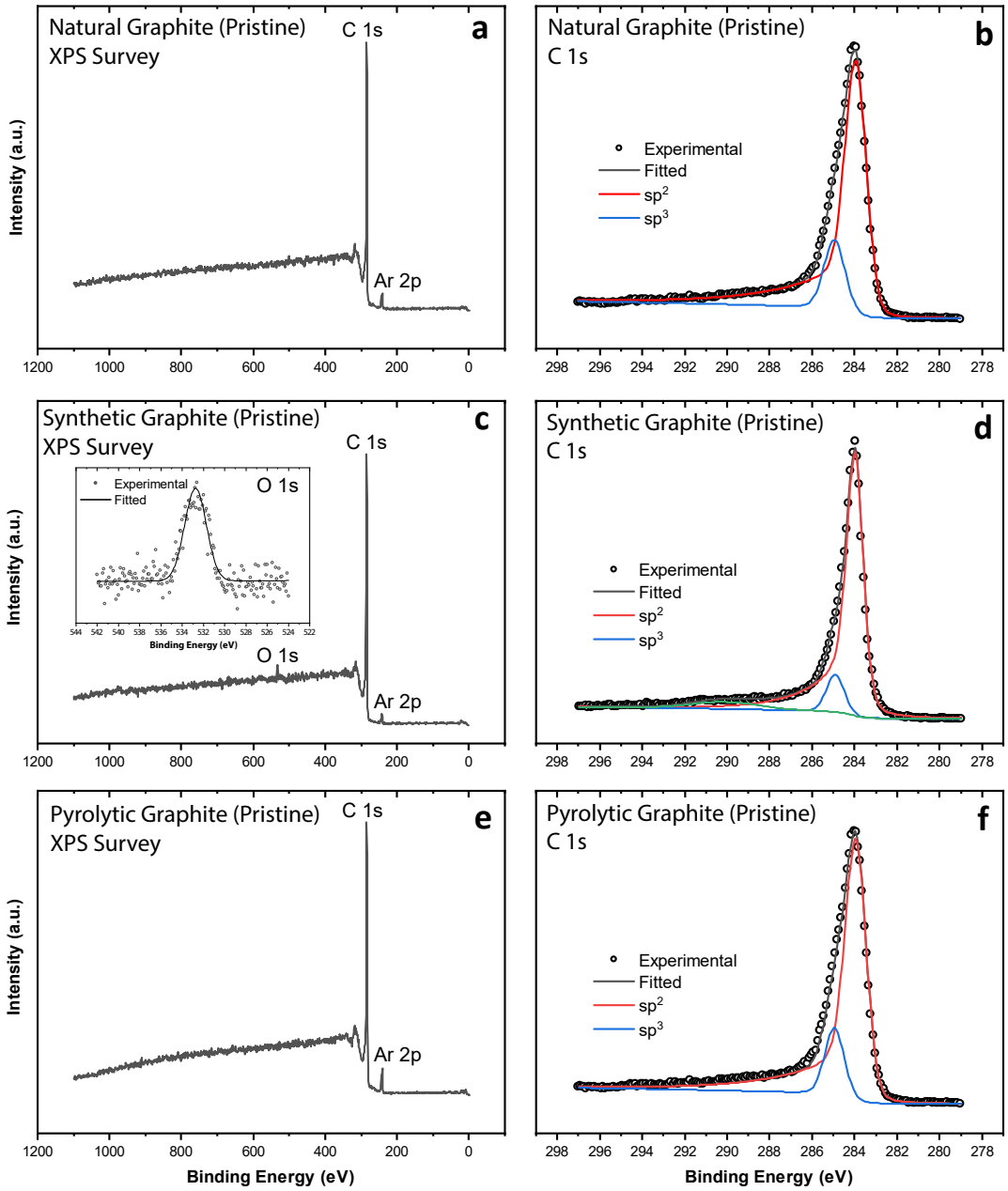

Figure S2. X-ray photoelectron (XPS) survey and deconvoluted C 1s spectra of pristine (a,b) natural graphite, (c,d) synthetic graphite (inset: fitted O 1s region), and (e,f) pyrolytic graphite. Concentrations (atomic %) are based on signal intergration of C 1s components are tabulated in Table S1.

Table S1. Concentrations of carbon and oxygen states obtained by quantitative deconvolution of XPS C 1s signals.

Graphite Type	Atomic %			Chi-squared (χ^2)
	C sp^2 (284.0 ± 0.1 eV)	**C sp^3** (285.0 ± 0.1 eV)	**C=O & O-C=O** (289.9 eV)	
Natural	85.2	14.8	-	1.95
Synthetic	84.3	9.0	6.7	5.37
Pyrolytic	83.9	16.1	-	2.38

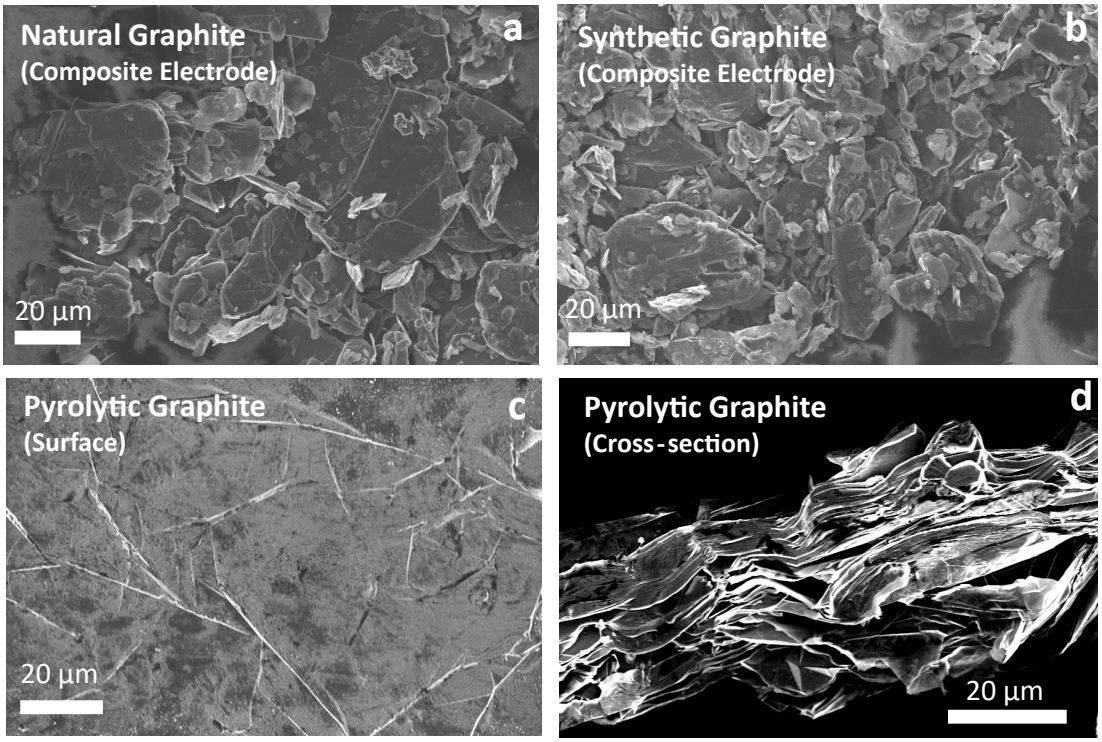

Figure S3. Scanning electron microscopy (SEM) images of a (a) natural graphite composite electrode, (b) synthetic graphite composite electrode, and (c,d) pristine pyrolytic graphite foil.

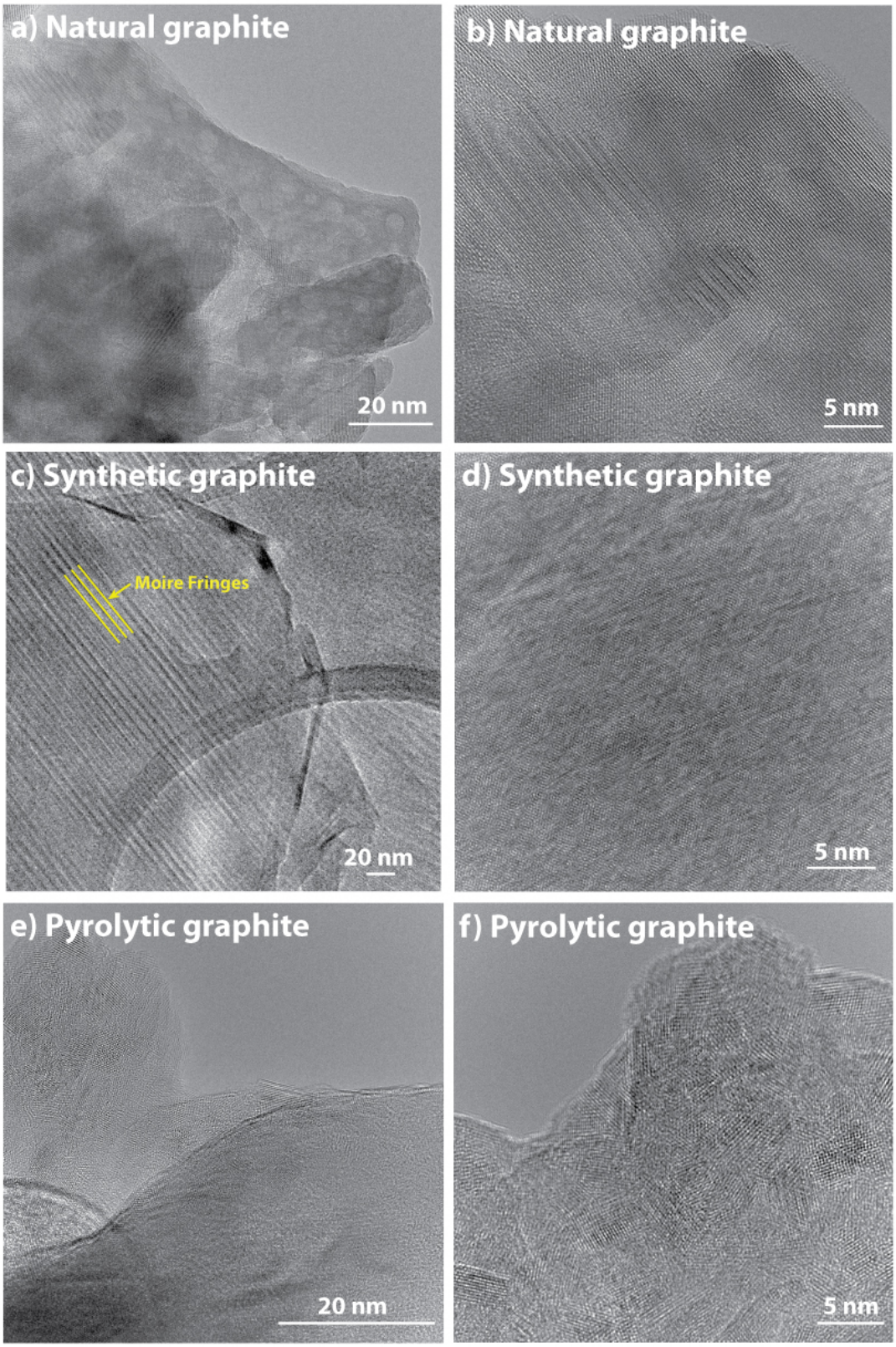

Fig S4. High-resolution transmission electron microscopy (HR-TEM) images showing the highly-ordered nanoscale structures of pristine (a,b) natural graphite, (c,d) synthetic graphite, and (e,f) pyrolytic graphite.

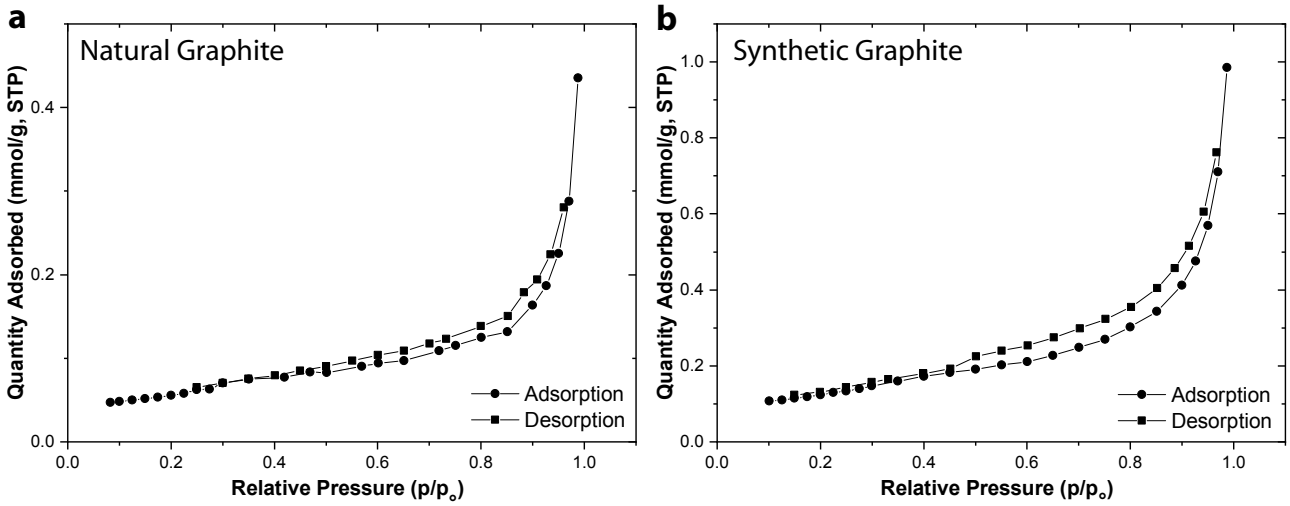

Figure S5. Nitrogen sorption isotherms for pristine (a) natural graphite and (b) synthetic graphite. No isotherm was obtained for pyrolytic graphite due to its low specific surface area, which was estimated via single-point BET analysis conducted at $P/P_0 = 0.3$.

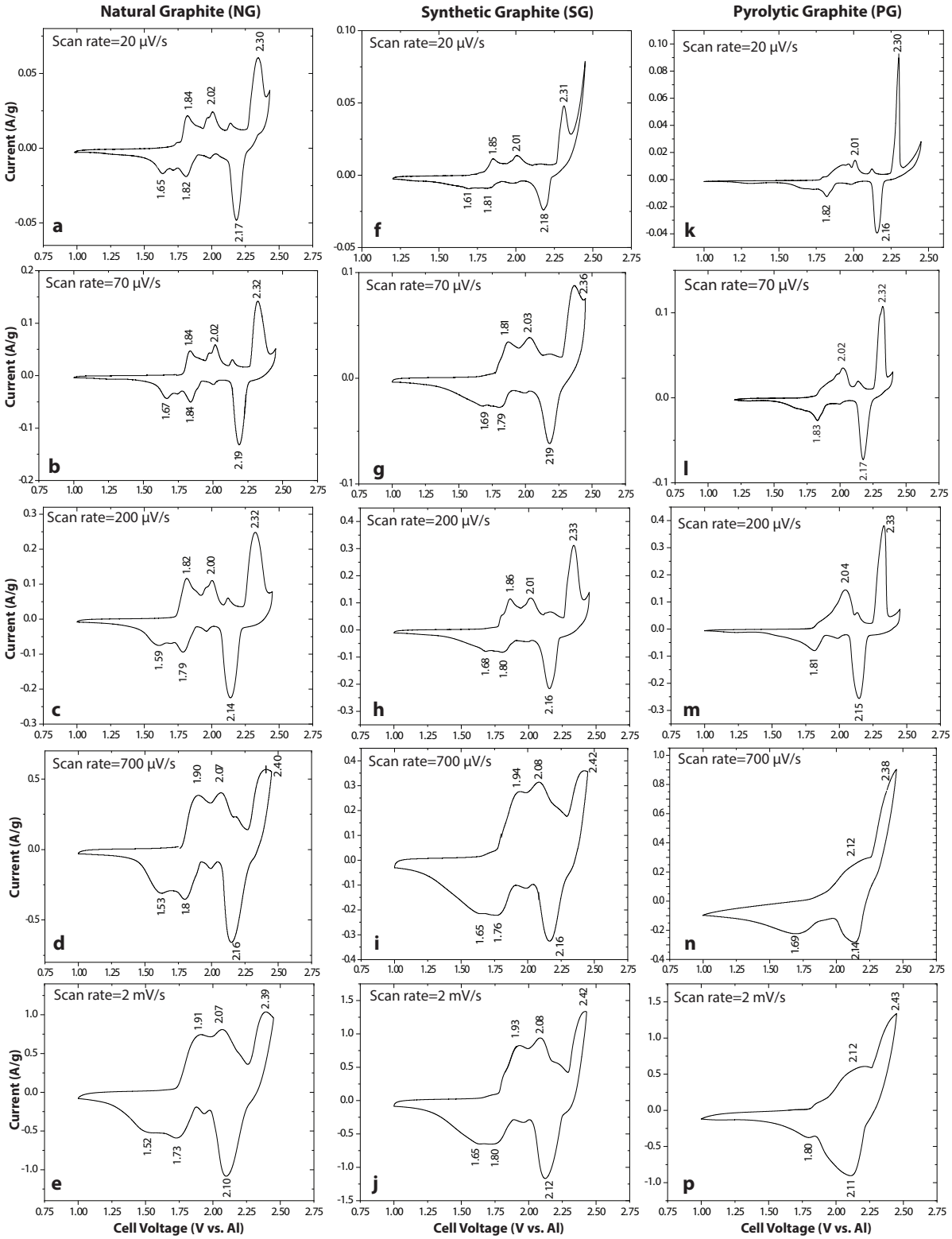

Figure S6. Variable scan-rate cyclic voltammograms (CVs) of representative Al-graphite cells with (a-e) natural graphite, (f-j) synthetic graphite, and (k-p) pyrolytic graphite at scan rates ranging from 20 μV/s to 2 mV/s.

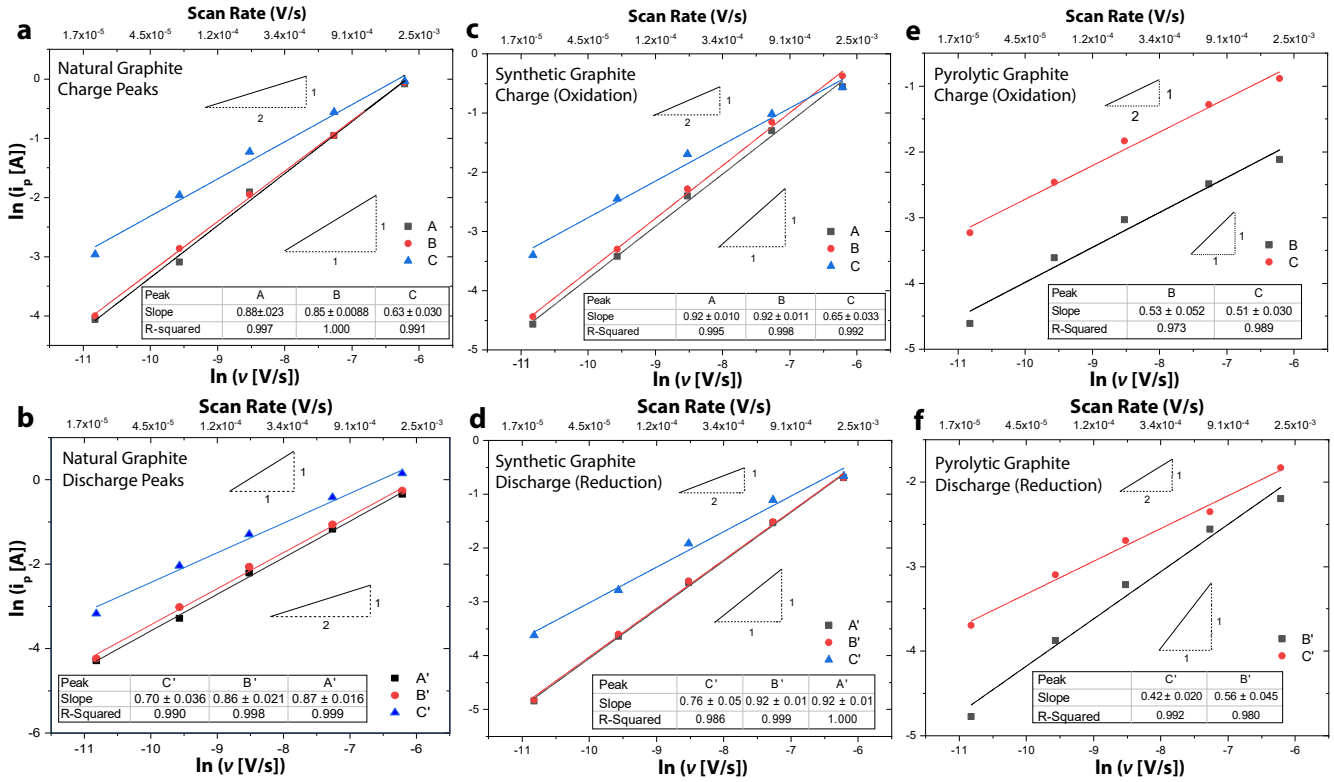

Figure S7. Variable-rate analyses of CV data for on Al-graphite cells with (a,b) natural, (c,d) synthetic, and (e,f) pyrolytic graphites. Peak current vs. scan rate data was fit to a power law model (Eqn. 3, main text). Exponential scaling term (*b*-value) for the oxidation and reduction peaks as a function of potential are shown as insets. Measurements were performed on three different cells for each graphite type; one representative trial is shown here.

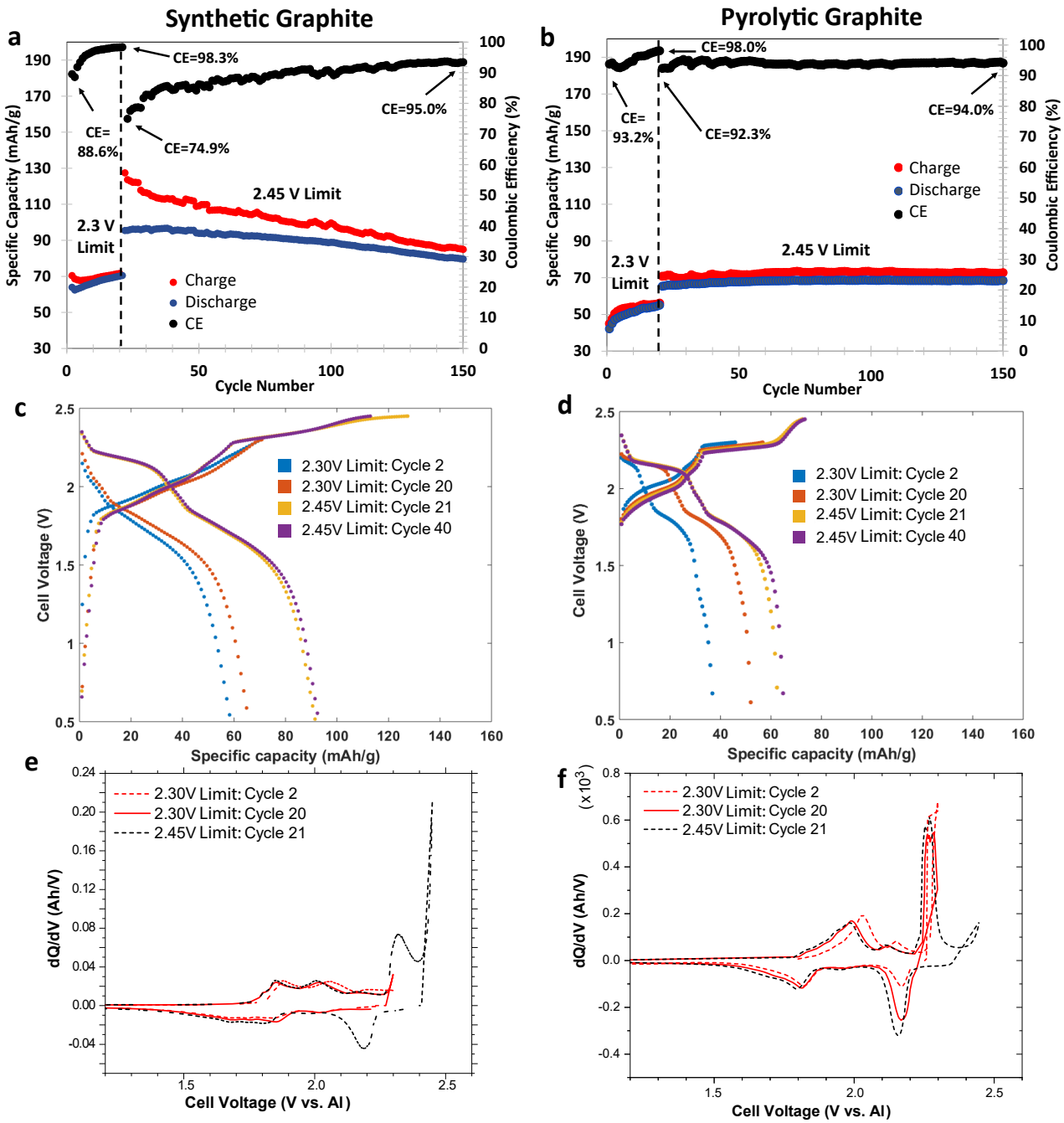

Figure S8. Electrochemical performance of Al-graphite cells with synthetic graphite (SG) and pyrolytic graphite (PG), where a reduced voltage limit of 2.30 V was used for the first 20 cycles and subsequently raised to 2.45 V on cycle 21 and after, improving long-term coulombic efficiency. (a,b) Galvanostatic cycling, (c,d) cyclic voltammetry, and (e,f) differential capacity (dQ/dV) plots are shown for (a,c,e) synthetic grahpite and (b,d,f) pyrolytic graphite.

Supporting Text & Calculations

Text S1. Calculation of the porosity of the composite electrodes:

The porosities of the composite natural & synthetic graphite composite electrodes were estimated according to:

$$\%\ Porosity = \left(1 - \left[\frac{\rho_{electrode}}{\rho_{graphite}}\right]\right) * 100$$

where $\rho_{electrode}$ and $\rho_{graphite}$ are the densities of the composite electrode and the pristine graphite material (e.g., ~2.1 g/cm^3 for natural graphite, specified by manufacturer), respectively. The density of the composite electrode, $\rho_{electrode}$, was obtained by measuring the mass of an electrode and dividing by its overall volume.

Text S2. Calculation of the theoretical interlayer surface area & comparison to measured external surface area:

Calculation of theoretical surface area of one side of a graphene layer[1]*:*

The unit cell of graphene is a two-dimensional rhombus that contains two carbon atoms and has an area of 0.052 nm^2. The mass of each unit cell is equal to the mass of two carbon atoms:

$$Mass\ of\ graphene\ unit\ cell\ = 2 * 12.011\ amu * \frac{1.6605*10^{-24}\ g}{1\ amu} = 3.99 * 10^{-23} g$$

Thus, the theoretical specific surface area of one side of a graphene layer is:

$$Theoretical\ specific\ surface\ area\ (one-side) = \frac{A}{M} = \frac{0.052\ nm^2}{3.99*10^{-23} g} = 1.31 * 10^{21}\ \frac{nm^2}{g} = 1315 \frac{m^2}{g}$$

Comparison of theoretical interlayer and measured "external" surface areas:

Accounting for the typical porosity (~40%) of a graphite electrode, the theoretical interlayer specific surface area is:

$$Theoretical\ specific\ surface\ area\ (one-side, porous)\ = (1 - 0.4)\left(1315 \frac{m^2}{g}\right) = 789\ \frac{m^2}{g}$$

The measured BET specific surface area of synthetic graphite (highest among the electrodes studied here) was 9.3 m^2/g. Thus, for synthetic graphite, the measured BET surface area is ~1.2% of the total graphene interlayer surface area (one-sided basis). The measured BET surface area for natural and pyrolytic graphites is 0.7% and 0.1% of the graphene interlayer surface area, respectively. This result establishes that the capacity achieved is dominated by electrochemical intercalation of chloroaluminate anions into the graphite interlayers, as opposed to surface phenomena (e.g., double-layer capacitance or electrochemical reaction of adsorbed species).

Text S3. Calculation of overall composition ($C_x[AlCl_4]$) of a fully-intercalated graphite electrode:

The average composition of an intercalated graphite electrode can be calculated from the discharge capacity per mass of graphite (mAh/g). For NG electrodes, one full discharge yields a capacity of 115 mAh/g, or in terms of number of electrons:

$$Number\ of\ AlCl_4^-\ anions\ transferred\ during\ one\ full\ discharge\ =$$

$$\left(\frac{115\ mAh}{g\ graphite}\right)\left(\frac{1\ mol\ e^-}{26800\ mAh}\right)\left(\frac{1\ mol\ AlCl_4^-}{1\ mol\ e^-}\right)\left(\frac{6.022*10^{23}\ molecules\ of\ AlCl_4^-}{1\ mol}\right) = \frac{2.59*10^{21}\ molecules\ of\ AlCl_4^-}{g\ graphite}$$

The above result can be used to calculate the average composition of the intercalated electrode just prior to discharging:

$$Average\ composition\ of\ NG\ electrode\ prior\ to\ discharging\ =$$

$$\left(\frac{2.59*10^{21}\ molecules\ of\ AlCl_4^-}{g\ graphite}\right)\left(\frac{1.995*10^{-23} g\ graphite}{1\ atom\ of\ C}\right) = \frac{0.0517\ molecules\ of\ AlCl_4^-}{1\ atom\ of\ C} \approx \frac{1\ molecule\ of\ AlCl_4^-}{19\ atoms\ of\ C}$$

Thus, the fully intercalated NG electrode has 1 $AlCl_4^-$ anions for every 19 C atoms, yielding an average composition of $C_{19}[AlCl_4]$. This result is similar to a comparable NG system studied by Elia *et al.*[2], who computed $C_{20}[AlCl_4]$. Performing the same calculation for SG and PG yields average compositions of $C_{28}[AlCl_4]$ and $C_{34}[AlCl_4]$, respectively.

The experimental capacity of the first charge of the natural graphite electrode is 160 mAh/g, which is higher than the discharge capacity of 115 mAh/g, likely due to a combination of irreversible electrochemical side reactions (e.g., electrolyte degradation) and intercalated $AlCl_4^-$ ions that become "trapped", i.e., unable to de-intercalate. It is informative to compute the average composition of the fully-charged NG electrode assuming that the additional 45 mAh/g observed on the first charge is due solely to trapped ions, which yields $C_{14}[AlCl_4]$. The actual average composition of the fully-charged natural graphite is thus somewhere between $C_{19}[AlCl_4]$ (neglecting ion trapping) and $C_{14}[AlCl_4]$.

Text S4. Estimation of theoretical capacity & ion stage numbers via Coulombic & geometric arguments.

Calculation of interlayer packing density and theoretical capacity of stage-1-intercalated graphite using hard-sphere model:

We first estimate the theoretical capacity of stage-1-intercalated graphite assuming the $AlCl_4^-$ ions to be rigid, non-interacting spheres (ionic diameter = 5.28 Å)[3] and maximum 2D hexagonal packing of circles (packing fraction of 0.907). The ratio of the cross-sectional area of $AlCl_4^-$ anions to the area of the graphene unit cell is:

$$Ratio\ of\ effective\ area\ of\ AlCl_4^-\ to\ graphene\ unit\ cell =$$

$$\frac{Area\ of\ AlCl_4^-\ /\ Fraction\ of\ occupied\ area}{Area\ of\ graphene\ unit\ cell} = \frac{0.219\ nm^2\ /\ 0.907}{0.0524\ nm^2} = 4.64\ \frac{Effective\ area\ of\ AlCl_4^-}{Area\ of\ graphene\ unit\ cell}$$

Thus, 4.64 graphene unit cells thus comprise the effective area (corrected for packing effects) of 1 $AlCl_4^-$ ion. Since each graphene unit cell has 2 carbon atoms, the maximum $AlCl_4^-$ concentration is $C_{9.3}[AlCl_4]$. Under these assumptions, the theoretical capacity at stage 1 can be computed:

$$Maximum\ capacity\ of\ stage\ 1\ AlCl_4^-\ intercalated\ graphite\ [hard-sphere\ model]\ =$$

$$\left(\frac{1\ molecule\ of\ AlCl_4^-}{9.3\ \ atom\ of\ C}\right)\left(\frac{1\ atom\ of\ C}{1.995*10^{-23} g\ graphite}\right)\left(\frac{1\ mol\ of\ AlCl_4^-}{6.022*10^{23}\ molecules\ of\ AlCl_4^-}\right)\left(\frac{1\ mol\ e^-}{1\ mol\ AlCl_4^-}\right)\left(\frac{26800\ mAh}{1\ mol\ e^-}\right) = 240\frac{mAh}{g\ graphite}$$

Estimates of theoretical capacity of stage-1-intercalated graphite using DFT models from literature:

The actual shape, dimensions and packing density of $AlCl_4^-$ ions within the graphite layers will depend strongly upon molecular-level interactions between the $AlCl_4^-$ ions and bounding graphene layers, as well as among the $AlCl_4^-$ ions themselves. Density functional theory (DFT) electronic structure calculations may yield more accurate results. However, the current literature indicates that a range of interlayer packing densities may be stable at different cell voltages. For example, using DFT methods, Gao et al.[4] found that packing 1 $AlCl_4^-$ ion per 2x2 or 3x3 repetition of the graphene unit cell yielded formation energies within 0.01 eV of each other, but that generally, higher interlayer packing densities are more energetically favorable than dilute ones (e.g., compared to 1 $AlCl_4^-$ ion per 4x4 repetition, or even more dilute). Considering only the single graphene layer that hosts the $AlCl_4^-$ ion, the 2x2 and 3x3 configurations correspond to compositions of $C_8[AlCl_4]$ and $C_{18}[AlCl_4]$, respectively, which for stage-1-intercalated graphite would result in theoretical capacities of 279 and 124 mAh/g, respectively. Thus, current DFT methods indicate that high interlayer packing densities are favorable and that a range of interlayer compositions may be possible.

Estimation of average stage number of fully-charged graphite based on a coulometric-geometric model:

The average stage number of the intercalated graphites can be estimated by comparing the average composition $C_x[AlCl_4]$, determined coulometrically from the experimentally measured capacity, to the theoretical composition at a given stage number and interlayer packing density. For example, the natural graphite studied here exhibited a discharge capacity of 115 mAh/g, or an overall composition of $C_{19}[AlCl_4]$ (Text S3). Assuming hard-sphere packing of $AlCl_4^-$ as a first approximation, stage-2-intercalated graphite would have a theoretical capacity of 120 mAh/g and an average composition of $C_{18.6}[AlCl_4]$. Natural graphite thus exhibits an experimental capacity and composition very close to the theoretical capacity and composition of stage-2-intercalated graphite using the hard-sphere model. Consideration of ion trapping would increase the expected $AlCl_4^-$ content and thus decrease the average stage number towards stage 1. For example, if all 160 mAh/g of the

first charge of NG were a result of the electrochemical intercalation of $AlCl_4^-$ ions, then the overall composition would be $C_{14}[AlCl_4]$ (Text S3), which would indicate a mixture of stage 1 and stage 2 intercalation based on the hard-sphere packing model. Furthermore, if models using lower interlayer packing densities of $AlCl_4^-$ ions are used, then the graphite would need to exhibit a lower stage number, on average, to hold the same overall concentration of $AlCl_4^-$ ions.

As highlighted in the main text, there are currently discrepancies between the stage numbers of fully-charged graphites determined by XRD methods, Raman spectroscopy, and coulometric-geometric models. Reconciling these discrepancies would provide opportunities to clarify the structure and composition of the chloroaluminate-intercalated graphite electrodes, as well as any role of defects and disorder.

References

(1) Bonaccorso, F.; Colombo, L.; Yu, G.; Stoller, M.; Tozzini, V.; Ferrari, A. C.; Ruoff, R. S.; Pellegrini, V. Graphene, Related Two-Dimensional Crystals, and Hybrid Systems for Energy Conversion and Storage. *Science* **2015**, *347*, 1246501.

(2) Elia, G. A.; Kyerematen, N. A.; Marquardt, K.; Hahn, R. An Aluminum/Graphite Battery with Ultra-High Rate Capability. *Batter. Supercaps* **2018**, *2*, 83–90.

(3) Takahashi, S.; Koura, N.; Kohara, S.; Saboungi, M.-L.; Curtiss, L. A. Technological and Scientific Issues of Room-Temperature Molten Salts. *Plasmas Ions* **1999**, *2*, 91–105.

(4) Gao, Y.; Zhu, C.; Chen, Z.; Lu, G. Understanding Ultrafast Rechargeable Aluminum-Ion Battery from First-Principles. *J. Phys. Chem. C* **2017**, *121*, 7131–7138.